

*The role of oscillatory  
synchronization in the decoding of  
temporal information in PN  
assemblies*

---

---

## *Abstract*

Synchronization of neuronal assemblies has been widely found in brain circuits. Its functional significance, however, remains a mystery. In the locust antennal lobe, PNs respond to odors with oscillatory synchronization. Synchronization is mediated by oscillatory inhibition and can be selectively disrupted with picrotoxin, a GABA antagonist (MacLeod and Laurent, 1996). We exploited this manipulation to test four hypotheses for the role of synchronization. We show that synchronization does not reduce PN firing rates and does not decorrelate PN responses in time. Furthermore, the informational value about odor identity of synchronized spikes is not different from that of unsynchronized spikes. Synchronization is nonetheless shown to be essential for the correct decoding of odor information in PN assemblies by downstream neurons. Disruption of synchronization leads to loss of odor-related information in downstream neurons. The informational value in the set of synchronized spikes is shown to be equivalent to that of the set of all spikes, suggesting that downstream neurons sensitive only to synchronized spikes do not miss information on odor identity.

---

## *Introduction*

This chapter employs a methodology adapted from work in the visual system for use in the olfactory system for the first time, and applies it to study two related problems stemming from previous work of the laboratory.

---

### *I. Picrotoxin does not alter stimulus information in PN spike trains*

Previous results claiming that picrotoxin selectively disrupts synchronization without affecting slow temporal patterns (MacLeod and Laurent, 1996) have been subject to the criticism that it appeared

---

arbitrary to say that the slow temporal patterns remained unaffected, given that some degree of change was present whose significance, relative to the variability inherent in neuronal responses, was unknown. Our present results show that an objective criterion, namely the stimulus information present in the spike trains, as measured by the fraction of trials assigned to the correct odor using closest-neighbor classification employing a cost-based metric, renders spike trains of single cells in control and picrotoxin-injected conditions statistically undistinguishable.

---

## *II. A role for neuronal synchronization*

As Lord Adrian pointed out in 1951, the fact that the differences in the spatial and temporal pattern of excitation produced by different smells can be distinguished by the electrophysiologist does not mean that smells are distinguished in this way by the animal (Adrian, 1951). This chapter provides evidence that, indeed, the olfactory system is unable to read information *present* in neuronal assemblies when those assemblies are desynchronized.

Synchronization is a ubiquitous phenomenon in brain circuits. It has long been known that the mammalian olfactory bulb exhibits oscillatory activity in response to odors (Adrian, 1950). Neurons in the visual system synchronize in response to visual objects (Gray and Singer, 1989). Synchronization has also been found in the somatosensory system (Nicoletis et al., 1995), the motor system (Riehle et al., 1997), the hippocampus (reviewed in Bland and Oddie, 2001) and frontal cortex (Abeles et al., 1993). Recent experiments suggested that synchronization serves a function in the discrimination of similar, but not dissimilar, odors by the bee (Stopfer et al., 1997). But what is this function that has remained elusive for so long?

---

One hypothesis for the role of synchronization is that the role of the inhibition is to reduce prolonged activity and thus prevent learning. If inhibition is prevented in the accessory olfactory bulb of rats by a bicuculline injection, an olfactory memory for the odor present is created (Brennan et al., 1990). This memory prevents pregnancy blocking by the odor (Brennan et al., 1990). This could potentially explain the lack of synchronizing inhibition in the first trial of exposure to an odor (Stopfer and Laurent, 1999): once an odor is not novel, learning is inhibited.

At the behavioral level, disruption of oscillatory inhibition did not lead to the creation of a more robust memory for the odors presented, but rather, to greater confusion between chemically similar odorants, and thus, presumably weaker memories (Stopfer et al., 1997). On the other hand, “stronger” memories could become more overlapping for similar odorants after disruption of inhibition, and explain the picrotoxin-induced confusion. The results reported in the paper included at the end of this chapter (Macleod et al., 1998), however, show that firing rates do not increase after the disruption of synchronization by picrotoxin (see Fig. 4d in the paper). Furthermore, the mean spike count in 50 msec windows is not affected by picrotoxin ( $p > 0.36$ , Wilcoxon ranksum test).

Whether or not synchronization’s role is in learning as opposed to perception, it is conceivable that oscillatory inhibition serves to decorrelate PN responses in time. Since PN responses are bursty (Figs. 4.10-4.13 and 4.17), and if excitation in PNs is enhanced by depolarization, periodic inhibition could serve to hyperpolarize PNs following excitation and prevent the formation of a burst, making the neuronal assembly active in successive cycles more different from one another. This hypothesis can be tested by comparing the correlation in time of PN responses with and without oscillatory

---

inhibition.

In fact, the opposite was true: the absolute differences in spike count between successive 50 msec windows were slightly but significantly lower in control trials than after picrotoxin injection (mean in controls =  $0.067 \pm 0.001$  spikes vs.  $0.072 \pm 0.001$  spikes after PCT injection,  $p < 0.008$ , Wilcoxon ranksum test). Together with the fact that mean spike counts are not affected (see above), this indicates that synchronization actually causes a slight increase in the correlation of successive 50 msec windows in PN spike trains. Fig. 5.1 shows the spike-triggered firing rate average in control and after PCT injection. Fig. 5.2 shows the correlation between the spike counts in successive 50 msec time windows in control and after PCT injection.

A third hypothesis sustains that synchronization serves as a filter to differentiate spikes with high informational content from spikes with low informational content ('noise'). To test this, I compared the informational content of synchronized spikes (defined by a phase variance of less than  $\pi$  radians; this synchronization threshold was selected so that an equal number of synchronized and unsynchronized spikes were present) versus that of unsynchronized spikes, by classifying spike trains consisting only of the corresponding spike type into the odor corresponding to the closest cluster (see methods, below, and Fig. 5.3). The fraction of trials correctly classified for each PN using synchronized spikes was not significantly different from that using an equal number of unsynchronized spikes (Fig. 5.4,  $p > 0.1$  for every T-value (10, 25, 50, 100, 250, 500, 1000, 2000 and Inf) and z-value (-15 and 1) combination tested,  $n = 46$  PNs, Wilcoxon ranksum test). This result is consistent with our previous result showing that odor information in PNs is not disrupted by desynchronization with PCT (see Nature paper below). A caveat must be noted in that the classification was

---

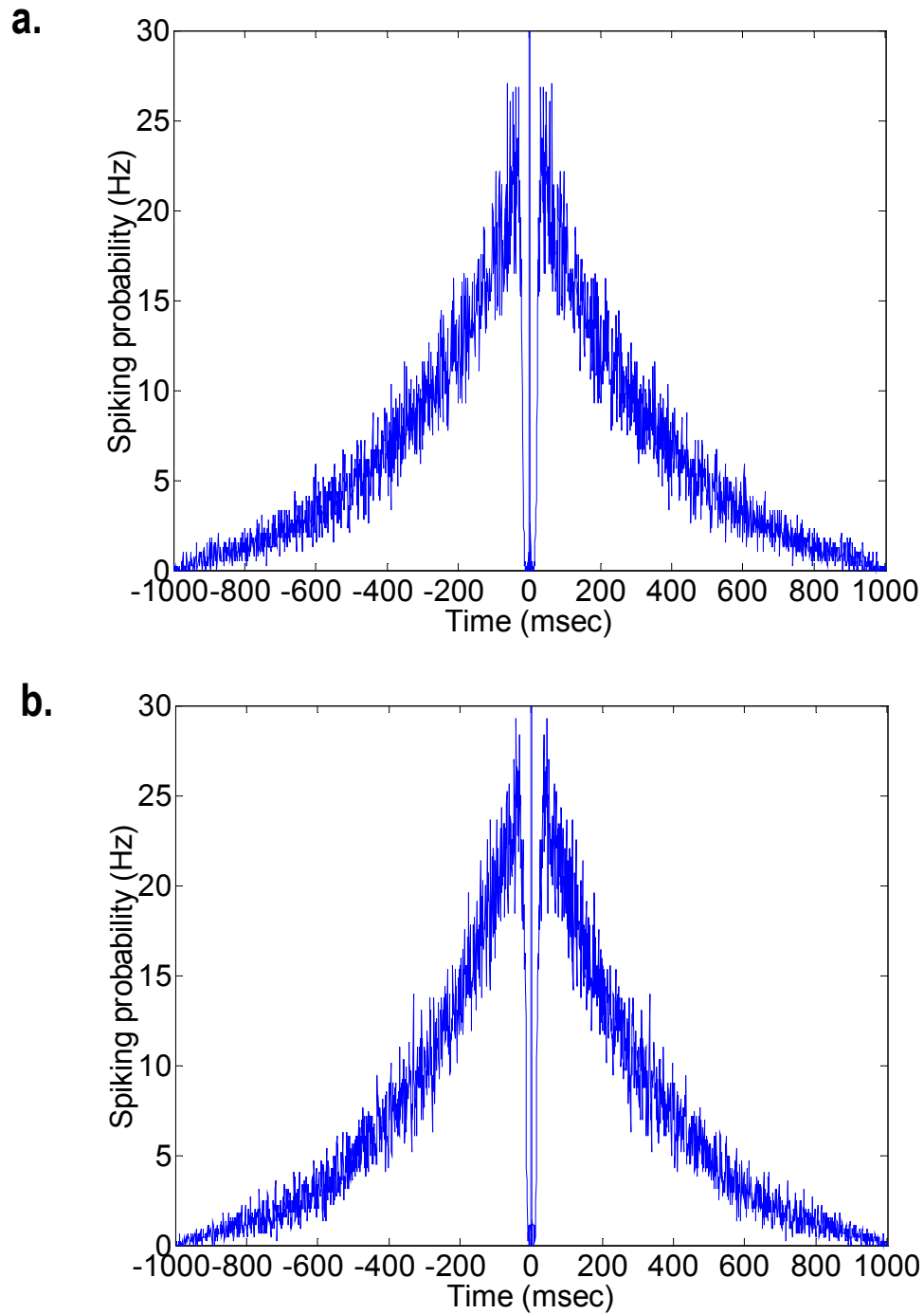
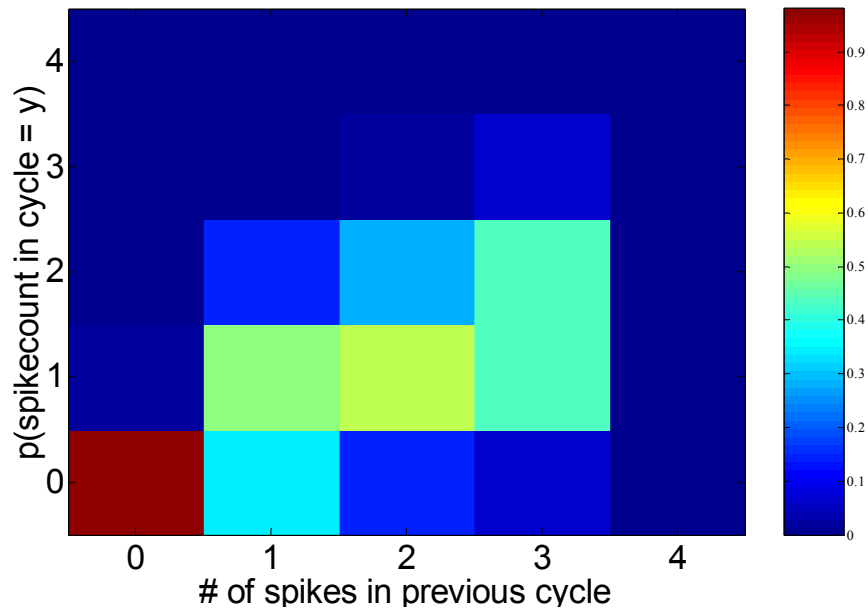


**Figure 5.1. Spike-triggered average firing rate before (a) and after (b) PCT injection.** Computed for the set of 12 PNs in Fig 4.11 (data courtesy of Katrina MacLeod).

a.



b.

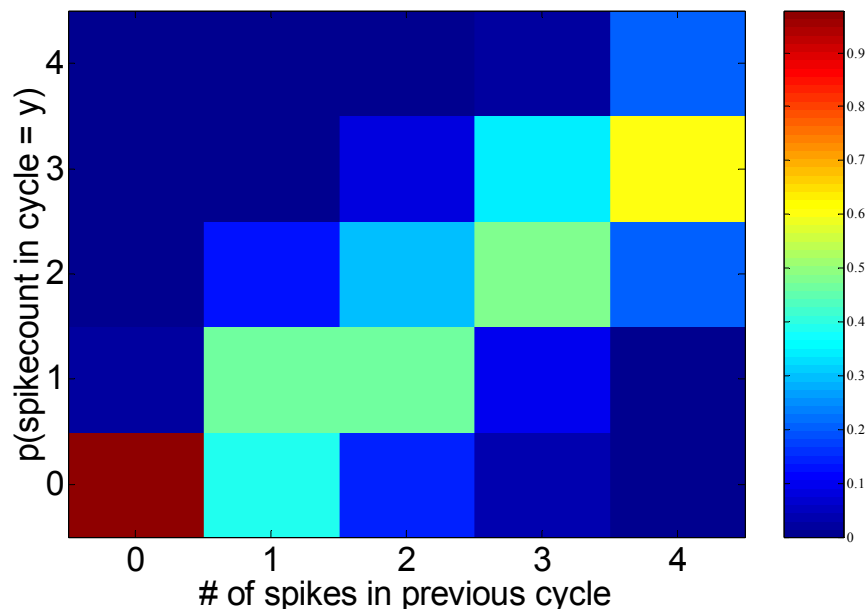
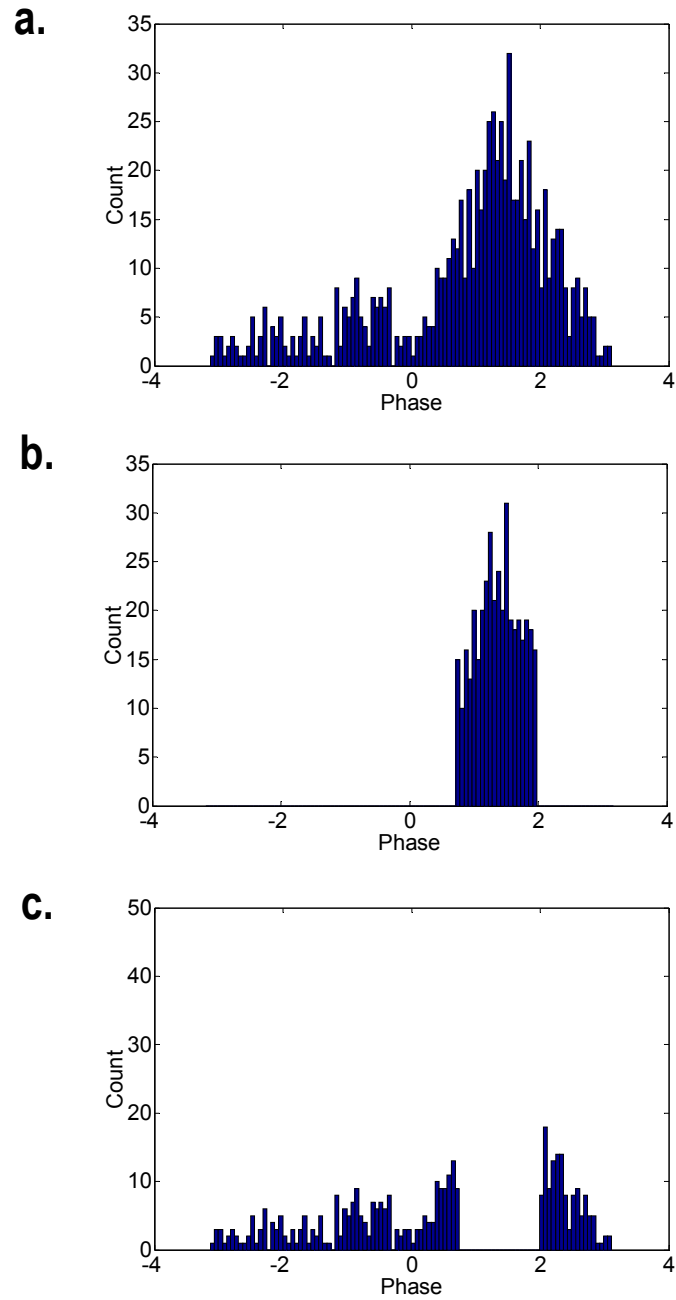


Figure 5.2. PN odor responses are bursty with and without synchronization: The probability of firing of a PN in any given cycle during the 3 sec following the onset of odor presentation before (a) and after (b) PCT injection is significantly enhanced if the PN has fired in previous cycles, and the number of spikes in successive cycles are significantly correlated.  $P(x,y) = p(\# \text{ of spikes in cycle } N=y \mid \# \text{ of spikes in cycle } N-1=x)$ . Computed for the set of 12 PNs in Fig. 5.1 (data courtesy of Katrina MacLeod).



**Figure 5.3. Method used to separate spikes into synchronized and unsynchronized spikes.** The entire phase distribution for the responses of a given PN-odor pair at a given concentration (a) is fed to an algorithm that calculates the mean (vector) phase and the phase range centered on the mean phase that divides all spikes in two sets with equal number of spikes. That closest to the mean phase is termed the synchronized half (b) and the other one is termed the unsynchronized one (c).

not performed simultaneously using spike trains from multiple PNs—a multi-cell analysis of a set of simultaneously recorded PNs is ongoing. The finding that, for single PNs, synchronized spikes are as informative as those which are not, however, suggests that synchronized spikes do not carry an intrinsic informational value higher than that of unsynchronized spikes.

Classification using synchronized spikes was itself not significantly different from classification using all spikes (Fig. 5.4,  $p > 0.04$  for every T-value (10, 25, 50, 100, 250, 500, 1000, 2000 and Inf) and z-value (-15 and 1) combination tested,  $n=46$  PNs, Wilcoxon ranksum test not corrected for multiple comparisons). This suggests that Kenyon cells do not miss out on odor information by reading out only synchronized spikes.

A final hypothesis holds that synchronization is important for downstream neurons to decode signals from neuronal assemblies, which may discard spikes unless they are part of a volley of quasi-simultaneous spikes across a cell assembly. In other words, even if synchronized spikes are not intrinsically more informative, they may be read out preferentially by the decoding algorithm employed by cells downstream of PNs. This hypothesis has recently garnered some support from the biophysics of Kenyon cells, which amplify large inputs nonlinearly (Pérez-Orive et al., in press).

The paper that follows, published in the October 15th 1998 issue of *Nature* and reproduced here with the kind consent of the publisher, examines this fourth hypothesis for the role of synchronization, and addresses the question of whether desynchronization impairs the information content of single PNs (see (I) above). The experimental work therein was carried out by Katrina MacLeod. My

---

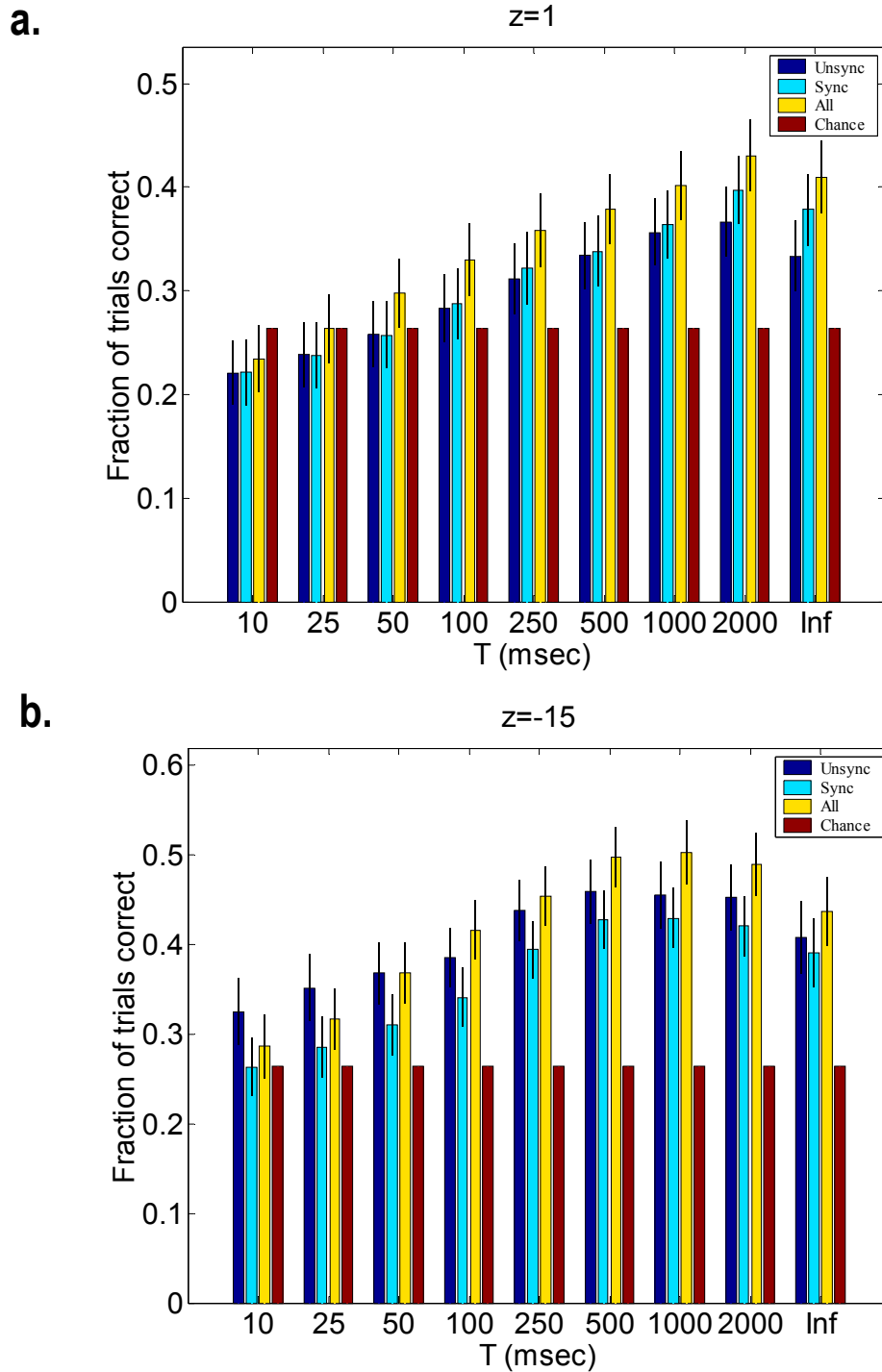


**Figure 5.4. Odor discrimination as a function of spike synchronization.** Mean fraction of trials correctly classified (and s.e.m.) by 46 PNs as a function of the timescale  $T$  of decoding (see Methods) using synchronized (light blue), unsynchronized (dark blue) or all (yellow) spikes, for (a) linear averaging across trials ( $z=1$ ) and (b) geometric averaging ( $z=-15$ ). Chance classification levels are shown in red.

contribution was limited to the proposal that a comparative information-theoretical analysis could help elucidate the initially puzzling effect of desynchronization of PNs on downstream neurons, and to the subsequent analysis that classified responses of PNs and downstream neurons into the odor responsible for eliciting the cluster most similar to each.

---

*A note on methods*

The paper employs two methods to classify spike trains into clusters corresponding to odors. Below is a brief comparison between the two. This may be of particular interest given that later papers (Stopfer and Laurent, 1999; Friedrich and Laurent, 2001; Bhazenov et al., 2001) have all employed the method that is less favored by the considerations below.

Differences between vector clustering method used by Katrina MacLeod (called #1 in the paper using a reverse chronological convention) and the clustering method using Victor and Purpura's cost-based metric I employed (#2) (MacLeod, Bäcker and Laurent, 1998):

## **A. Theory**

1. #1 uses binning, which results in general in a loss of resolution. This can be solved by applying convolution of the spike train with a gaussian prior to binning.
  2. #1 used an average spike train template, which may not be typical at all (as a crude example, the average of the points on a circumference does not lie in the circumference at all). #2 avoids having
-

to do that and looks at the distances between all individual spike trains. This could also be implemented for #1, though.

3. #1 was used in a pairwise comparison, while #2 was applied to a more difficult task that is closer to what the animal needs to do: choosing among all odors experienced.

4. Centroids including the spike train being classified, as done with method #1, eliminate independence of the classification because the distance is biased toward the right answer through the self-inclusion. This can be remedied by recalculating the centroid for each classification, excluding the corresponding spike train for each. Even better, centroids can be done without altogether (see #2 above).

5. The main and irreconcilable difference is that #2 takes the continuous nature of spike trains into account, while #1 deforms the one-dimensional nature of spike trains by mapping time bins onto Euclidean space. In doing so, #1 treats each bin as orthogonal to each other. Consequently, two spike trains with one spike each, in which one spike falls in one bin and the other in an adjacent bin, are just as different for method #1 as two spike trains with single spikes many seconds apart. In #2, in contrast, the distance between spike trains is directly related to the time difference between corresponding spikes.

## **B. Empirical comparison**

A comparison of the results yielded by the vector clustering algorithm and the Victor and Purpura method (V&P) for the data in the paper below yields a simple yardstick by which to measure both methods (see Fig. 4b and c in the paper). For both PNs and  $\beta$ -lobe neurons, the answer of the clas-

---

sification method using V&P's distance seems to agree more with our visual inspection of the data and the results we reported in the paper than the vector-based one: For  $\beta$ -LNs, V&P is more sensitive in picking up the changes induced by picrotoxin (PCT), yielding a p-value twenty times smaller (i.e. more significant) than the vector method, even though V&P significance was assayed with a two-tailed test which is more conservative than the one-tailed test used for the vector method in that it does not assume that classification can only be impaired by PCT. This advantage of the V&P method in sensitivity was present despite the fact that V&P was applied to all datasets, while the vector method was applied only to datasets which showed good odor classification in the controls, a selection bias that, if anything, would tend to *increase* the impairment in correct classification due to PCT.

For PNs, V&P is able to classify PN responses just as well for PCT as for the controls ( $p=0.93!$ ), but the vector method yields a clearly visible, yet not significant, decrease in correct classification. Without any extra information, it is impossible to determine which of these represents the data more closely. This is not made any easier by the fact that the cluster method was applied to pairwise classification, while the V&P method was used to classify among all odors to which the neuron was exposed, so the fraction of trials correctly classified cannot be compared between the two. The visual inspection we later made of the data suggested to us, however, that the information in PNs to discriminate odors was unchanged by PCT application. Once again, the datasets used with the vector method were a selected subset, advancing a potential explanation for the nonsignificant decrease in information seen with that method but absent in the analysis with the V&P method that included all datasets.

The most biologically relevant alternative, of course, were our knowledge complete, would be to use the actual decoding algorithm of the neurons that constitute the real decoders of PNs and  $\beta$ -LNs.

---

stereo plaids appeared in separate 180-ms intervals separated by a 400-ms blank period. Observers selected the interval containing the more distant of the two test plaids. The plaids consisted of a 15° positive-disparity grating and a 45° zero-disparity grating, each with 5% contrast. They appeared at slightly different depths on the near side of the plane of fixation, as shown in Fig. 4. The two 15° gratings had disparity phase angles of 31.0° and 18.6°, yielding a horizontal disparity difference of 8'. The disparity of the adapting pattern was either midway between the disparities of the 15° component gratings appearing in the two test intervals or midway between the disparities of the 2D features appearing in the two test intervals. There were four adapting stimuli: a 15° grating, a 105° grating, a plaid with components at 15° and 45°, and a plaid with components at 105° and 135°. The horizontal disparities of the adaptors were set to correspond to the depths of adaptors A and B in Fig. 4. For plaid adaptors, both components (and the 2D features) had the same horizontal spatial disparity. Adapting gratings had spatial frequencies of 1.0 cycle per deg, the same as the test gratings; they appeared in a circular window with a diameter of 9°, to ensure complete retinal overlay of the 7.85° test window. Each run of 20 trials began with an adapting period of 40 s, and each trial began with a 4 s 'topping-off' adaptation period, with 0.4 s separating adaptor offset and the first test interval. Adaptors underwent smooth harmonic motion at 1.0 cycle per s to minimize retinal adaptation. Adaptation and no-adaptation conditions were identical except for the adaptor grating contrast (10 and 0%, respectively). Adaptor contrast and duration were identified by systematic sampling to favour disparity adaptation at the expense of contrast adaptation; relatively brief and low-contrast adaptors tended to yield this result. Contrast adaptation and disparity adaptation have opposite expected consequences, the former inhibiting and the latter facilitating depth discrimination. Observers were instructed to maintain fixation on the central square throughout each trial and to respond by clicking one of two on-screen buttons to indicate the interval containing the test plaid more distant from the observer. Of three observers, one was naive; all had corrected-to-normal monocular and stereo acuities. Each data point was based on 40 trials.

Received 21 November 1997; accepted 31 July 1998.

1. Wheatstone, C. Contributions to the physiology of vision. Part the first. On some remarkable, and hitherto unobserved, phenomena of binocular vision. *Phil. Trans. R. Soc. Lond. B* **2**, 371–393 (1838).
2. Ogle, K. N. *Researches in Binocular Vision* (Saunders, Philadelphia, 1950).
3. Bishop, P. O. *Neurosciences Research Study Program Boulder Symposium* (ed. Schmitt, F. O.) (Rockefeller Univ. Press, New York, 1970).
4. Julesz, B. *Foundations of Cyclopean Perception* (Univ. of Chicago Press, 1971).
5. Wallach, H. *On Perception* (ed. Wallach, H.) (Quadrangle, New York, 1976).
6. Farell, B. & Ahuja, S. Binocular disparity of 1- and 2-D contours. *Invest. Ophthalmol. Vis. Sci.* (suppl.) **37**, 284 (1996).
7. Farell, B. Depth coherence and depth reversal in stereo plaids. *Invest. Ophthalmol. Vis. Sci.* (suppl.) **38**, 904 (1997).
8. Ramachandran, V. S. & Cavanagh, P. Subjective contours capture stereopsis. *Nature* **317**, 527–531 (1985).
9. Schumer, R. A. & Ganz, L. Disparity averaging in random dot stereopsis. *J. Opt. Soc. Am.* **69**, 1479 (1979).
10. Stevenson, S. B. & Schor, C. M. Human stereo matching is not restricted to epipolar lines. *Vision Res.* **37**, 2717–2723 (1997).
11. Morgan, M. J. & Castet, E. The aperture problem in stereopsis. *Vision Res.* **39**, 2737–2744 (1997).
12. Adelson, E. H. & Movshon, J. A. Phenomenal coherence of moving visual patterns. *Nature* **300**, 523–525 (1982).
13. DeAngelis, G. C., Ohzawa, I. & Freeman, R. D. Depth is encoded in the visual cortex by a specialized receptive field structure. *Nature* **352**, 156–159 (1991).
14. Blakemore, C. & Hague, B. Evidence for disparity detecting neurons in the human visual system. *J. Physiol. (Lond.)* **225**, 437–455 (1972).
15. Hibbard, P. B. & Langley, K. Plaid slant and inclination thresholds can be predicted from components. *Vision Res.* **38**, 1073–1084 (1998).
16. von Helmholtz, H. *Treatise on Physiological Optics* Vol. 3 (ed. Southall, J. P. C.) (translated from German 3rd edn) (Optical Society of America, 1925).
17. Gillam, B., Chambers, D. & Lawergren, B. The role of vertical disparity in the scaling of stereoscopic depth perception: an empirical and theoretical study. *Percept. Psychophys.* **44**, 473–483 (1988).
18. Rogers, B. J. & Bradshaw, M. F. Vertical disparities, differential perspective and binocular stereopsis. *Nature* **361**, 253–255 (1993).
19. Hubel, D. H. & Wiesel, T. N. Receptive fields, binocular interaction and functional architecture in the cat's visual cortex. *J. Physiol. (Lond.)* **160**, 106–154 (1962).
20. Barlow, H. B., Blakemore, C. & Pettigrew, J. D. The neural mechanism of binocular depth discrimination. *J. Physiol. (Lond.)* **193**, 327–342 (1967).
21. Poggio, G. F. & Fischer, B. Binocular interaction and depth sensitivity in striate and prestriate cortex of behaving rhesus monkey. *J. Neurophysiol.* **40**, 1392–1405 (1977).
22. Zeki, S. Functional specialization and binocular interaction in the visual areas of rhesus monkey prestriate cortex. *Proc. R. Soc. Lond. B* **204**, 379–397 (1979).
23. Ferster, D. A comparison of binocular depth mechanisms in area 17 and 18 of the cat visual cortex. *J. Physiol. (Lond.)* **311**, 623–655 (1981).
24. LeVay, S. & Voigt, T. Ocular dominance and disparity coding in cat visual cortex. *Vis. Neurosci.* **1**, 395–414 (1988).
25. Nikara, T., Bishop, P. O. & Pettigrew, J. D. Analysis of retinal correspondence by studying receptive fields of binocular single units in cat striate cortex. *Exp. Brain Res.* **5**, 353–372 (1968).

26. Anzai, A., Ohzawa, I. & Freeman, R. D. Neural mechanisms underlying binocular fusion and stereopsis: Position vs. phase. *Proc. Natl Acad. Sci. USA* **94**, 5438–5443 (1997).
27. Mayhew, J. E. W. & Frisby, J. P. Stereopsis masking in humans is not orientationally tuned. *Perception* **7**, 431–436 (1978).

**Acknowledgements.** I thank D. C. Moore for laboratory assistance, and S. Ahuja, R. van Ee, J. Krauskopf, D. Matza, D. G. Pelli and S. B. Stevenson for comments and discussion.

Correspondence and requests for materials should be addressed to B.F. (e-mail: bart\_farell@isr.syr.edu).

## Who reads temporal information contained across synchronized and oscillatory spike trains?

Katrina MacLeod, Alex Bäcker & Gilles Laurent

California Institute of Technology, Division of Biology 139-74, Pasadena, California 91125, USA

Our inferences about brain mechanisms underlying perception rely on whether it is possible for the brain to 'reconstruct' a stimulus from the information contained in the spike trains from many neurons<sup>1–5</sup>. How the brain actually accomplishes this reconstruction remains largely unknown. Oscillatory and synchronized activities in the brain of mammals have been correlated with distinct behavioural states or the execution of complex cognitive tasks<sup>6–11</sup> and are proposed to participate in the 'binding' of individual features into more complex percepts<sup>12–14</sup>. But if synchronization is indeed relevant, what senses it? In insects, oscillatory synchronized activity in the early olfactory system seems to be necessary for fine odour discrimination<sup>15</sup> and enables the encoding of information about a stimulus in spike times relative to the oscillatory 'clock'<sup>16</sup>. Here we study the decoding of these coherent oscillatory signals. We identify a population of neurons downstream from the odour-activated, synchronized neuronal assemblies. These downstream neurons show odour responses whose specificity is degraded when their inputs are desynchronized. This degradation of selectivity consists of the appearance of responses to new odours and a loss of discrimination of spike trains evoked by different odours. Such loss of information is never observed in the upstream neurons whose activity is desynchronized. These results indicate that information encoded in time across ensembles of neurons converges onto single neurons downstream in the pathway.

The function of oscillations and synchronization in information processing, perception and action is difficult to establish directly. Studies in mammals have correlated the degree of neural synchronization with specific behavioural or cognitive tasks, such as segmentation<sup>8</sup>, rivalry<sup>9</sup>, and sensorimotor tasks<sup>10,11</sup>, suggesting a functional link. In locusts, stimulation by odours evokes synchronized firing in dynamic and odour-specific ensembles of projection neurons in the antennal lobe, a region analogous to the vertebrate olfactory bulb<sup>16–18</sup>. This synchronization relies critically on fast GABA ( $\gamma$ -aminobutyric acid)-mediated inhibition, and can be selectively blocked by local injection of the GABA receptor antagonist picrotoxin<sup>19</sup>. Picrotoxin spares the slow modulation of individual projection neuron responses<sup>19</sup> but desynchronizes the firing of the odour-activated assemblies<sup>19</sup> and impairs fine odour discrimination<sup>15</sup>. These results establish a causal link between synchronization and perception. They do not, however, determine where information is lost when projection neurons—the information channels—are desynchronized. One possibility is that no single neuron between sensory and motor/cognitive areas is, on its own, sensitive to input synchronization. The behavioural deficit caused

by desynchronization of projection neurons induced by picrotoxin would thus be a result of collective neural activity only. Another possibility is that injection of picrotoxin leads to a loss of information in the responses of individual projection neurons due, for example, to jittering in their spike times. Desynchronization of projection neurons would thus be a by-product of picrotoxin treatment, but not the actual cause of the behavioural deficit. Finally, perhaps individual projection neuron responses undergo no loss of information after picrotoxin treatment, but responses of neurons downstream from them do. This result would indicate that information contained across projection neurons<sup>16</sup> is indeed crucial, and it would identify the downstream neurons as decoders of this relational/temporal information.

We searched for such putative neural elements downstream from the antennal lobe projection neurons, which project to the mushroom body, where they make divergent connections onto ~50,000 mushroom body intrinsic neurons (Fig. 1a). Odours cause oscillatory activity in these neurons, but they evoke spiking responses only in very sparsely distributed ones<sup>20</sup>, making the sampling of odour-responsive neurons very difficult. We thus focused on a smaller population of neurons directly postsynaptic to the intrinsic neurons of the mushroom body<sup>21,22</sup>, two synapses downstream from the projection neurons (Fig. 1b). These neurons, the  $\beta$ -lobe neurons, receive convergent input from thousands of mushroom body intrinsic neurons and have clear odour-specific responses (Fig.

1c–e). This makes them a suitable ‘read-out’ of signals processed in the early olfactory system. We recorded intracellularly from the dendrites of these  $\beta$ -lobe neurons. Dye injection showed discrete and dense (presumed dendritic) arbors in the  $\beta$ -lobe and sometimes also within the pedunculus (Fig. 1b, left). Sparser, varicose (presumed axonal) fibres projected to the  $\alpha$ -lobe and sometimes also within the pedunculus (Fig. 1b, left). Many morphological types were found, indicating a heterogeneous population. Morphologically identical examples of a type (for example, Fig. 1b, left) could have different physiological profiles in different animals, indicating either many exemplars of a type in each animal, or an animal-specific tuning history. Many, though not all,  $\beta$ -lobe neurons responded to at least some of the ten odours that we presented and about half of them showed significant phase-locking of their spikes to the odour-evoked local field potential (LFP) oscillations. Responses were usually stimulus-specific but less complex than those of the projection neurons of the antennal lobe<sup>18</sup>. They consisted of phasic or phasotonic increases in firing rate and, in a few cases, of a suppression of firing (Fig. 1c–f). Whereas spiking responses could be brief, a subthreshold synaptic drive consisting of both excitatory and inhibitory postsynaptic potentials (EPSPs and IPSPs) was usually maintained throughout the duration of the stimulus and mushroom body LFP oscillation (Fig. 1e).

To determine whether responses of the  $\beta$ -lobe neurons depend on synchronization of the projection neurons, a  $\beta$ -lobe neuron was

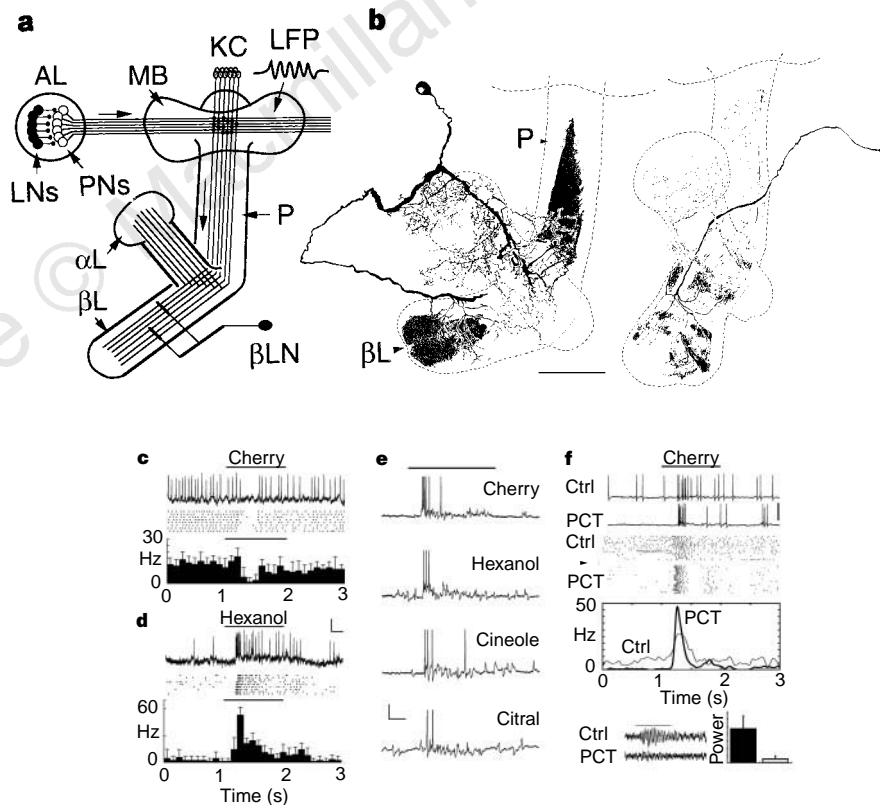


**Figure 1**  $\beta$ -lobe neurons ( $\beta$ LN). **a**, The insect olfactory pathways. Antennal lobe (AL) projection neurons (PNs) receive excitatory input from peripheral olfactory receptor neurons and GABA-mediated inhibitory input from local neurons (LNs)<sup>19,25</sup>. PNs project to the mushroom body (MB) calyx, where oscillatory local field potentials (LFPs) can be recorded in response to odours. Intrinsic neurons of the MB (the Kenyon cells, KCs) receive direct excitatory input from PNs<sup>20,25</sup>, and bifurcate to the  $\alpha$ - and  $\beta$ -lobes ( $\alpha$ L,  $\beta$ L)<sup>20</sup>.  $\beta$ LN receive input from thousands of KCs. **b**, Left and right, cobalt hexamine fills of two  $\beta$ LN, each from a different animal. P, pedunculus of the MB. Calibration, 100  $\mu$ m. **c**, Suppression of activity of

the left  $\beta$ LN in **b** in response to a cherry odour. Top, intracellular; centre, rasters; bottom, PSTH; mean firing  $\pm$  s.d. All odour pulses lasted for 1 s; 7–10 s between trials. Calibrations, 5 mV, 0.2 s. **d**, Prolonged excitatory response of the right  $\beta$ LN in **b** in response to the odour hexanol. Calibrations, 2 mV, 0.2 s. **e**, Transient excitatory responses of a third  $\beta$ LN to four odours. Note subthreshold activity during stimulus. Calibrations, 10 mV, 0.2 s. **f**, Effect of picrotoxin injection on a fourth  $\beta$ LN. Top to bottom: intracellular, rasters, smoothed PSTHs, LFP (bottom left), and normalized integrated power of LFP (bottom right) over 15–30 Hz, mean  $\pm$  s.d., before (black) and after (open) picrotoxin injection. Calibration, 50 mV.

impaled and its odour tuning characterized. PicROTOXIN was injected into the ipsilateral antennal lobe and the induced PN desynchronization was verified from the power spectrum of the ipsilateral mushroom body LFPs<sup>19</sup>. The responses of the  $\beta$ -lobe neurons to odours were then tested again. We made three main observations ( $n = 19$   $\beta$ -lobe neurons). First, picROTOXIN-induced desynchronization of projection neurons never abolished those  $\beta$ -lobe neuron odour responses that existed before injection of picROTOXIN ( $n = 15$   $\beta$ -lobe neurons). Second, desynchronization of projection neurons often caused changes in some, though not all existing  $\beta$ -lobe neuron odour responses. These changes consisted of a decrease in baseline firing rates ( $n = 6$   $\beta$ -lobe neurons), or a combined increase in the response and a decrease in the spontaneous firing rates ( $n = 4$   $\beta$ -lobe neurons), resulting in a more 'sculpted' response than in pre-picROTOXIN controls (Fig. 1f). In many cases, injection of picROTOXIN caused a change in the temporal patterning of the  $\beta$ -lobe neuron odour response ( $n = 14$   $\beta$ -lobe neurons) (see below). Third, desynchronization of the projection neurons could induce a  $\beta$ -lobe neuron to respond to odours to which it was previously not tuned (Fig. 2). Such picROTOXIN-induced changes occurred in five  $\beta$ -lobe neurons and in nine odour–neuron combinations out of the fourteen tested; for example, a  $\beta$ -lobe neuron could, after desynchronization of the projection neurons, acquire a response to one odour and not to another. This selectivity was observed in four of the five  $\beta$ -lobe neurons. Such picROTOXIN-induced responses were never observed in antennal lobe projection neurons ( $n = 10$  projection neurons). In summary, some changes induced in  $\beta$ -lobe neurons by injection of picROTOXIN into the antennal lobe consisted of the appearance of *de novo* odour sensitivity, thus decreasing the

neuron's selectivity. Other changes (in 58 per cent of all neurons and 34 per cent of all odour–neuron pairs tested) were more subtle and consisted of a modification of existing responses to a set of odours (see below).

Consider a  $\beta$ -lobe neuron that shows different response patterns to each of three odours, A, B and C. Desynchronization of the projection neurons often caused the responses to A, B, and C (or to a pair of these odours) to become more similar to each other, thus decreasing the likelihood of correct odour identification using the information contained in each spike train. We used two clustering algorithms to quantify the effect of picROTOXIN treatment on  $\beta$ -lobe neuron response classification. These algorithms categorize trials and assign each one to an odour on the basis of similarity between spike trains (see Methods). An example is shown in Fig. 3a, in which desynchronization of projection neurons caused a considerable loss in the specificity of the  $\beta$ -lobe neuron response to three related aliphatic alcohols. This classification (Fig. 3b) was carried out with pairwise comparisons of all pre-picROTOXIN trials (Fig. 3c, top row) and indicated a complete discriminability (Fig. 4a, left). PicROTOXIN was injected into the ipsilateral antennal lobe and classification was repeated; that is, each response was attributed a probable stimulus given its proximity to any of the three pre-picROTOXIN templates. The

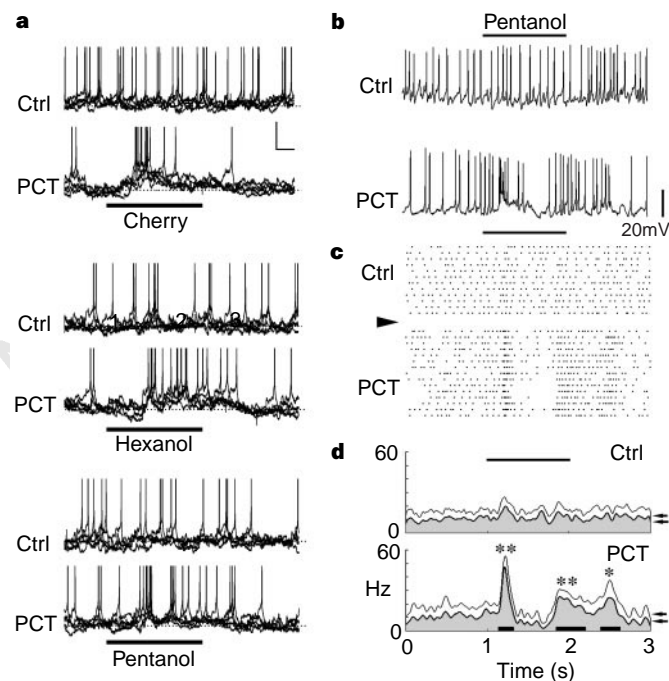


**Figure 2** Induction of odour-evoked responses in  $\beta$ -lobe neurons ( $\beta$ LN) after injection of picROTOXIN (PCT) into the antennal lobe. **a**, Five superimposed intracellular traces from one  $\beta$ LN before (Ctrl) and after PCT injection, for three different odours. Dotted line, resting membrane voltage. Calibrations: 5 mV, 0.2 s. **b–d**, Measurements from a different  $\beta$ LN. **b**, Intracellular traces. **c**, Rasters. **d**, Smoothed PSTH. Although there was no response to pentanol in the control, this  $\beta$ LN developed a response to this odour after PCT injection. Shaded PSTH represents mean rate; thin line represents s.d. Dark bars at bottom represent epochs in which the firing rate is significantly different from control. \*\* $P < 0.01$ ; \* $P < 0.05$ .

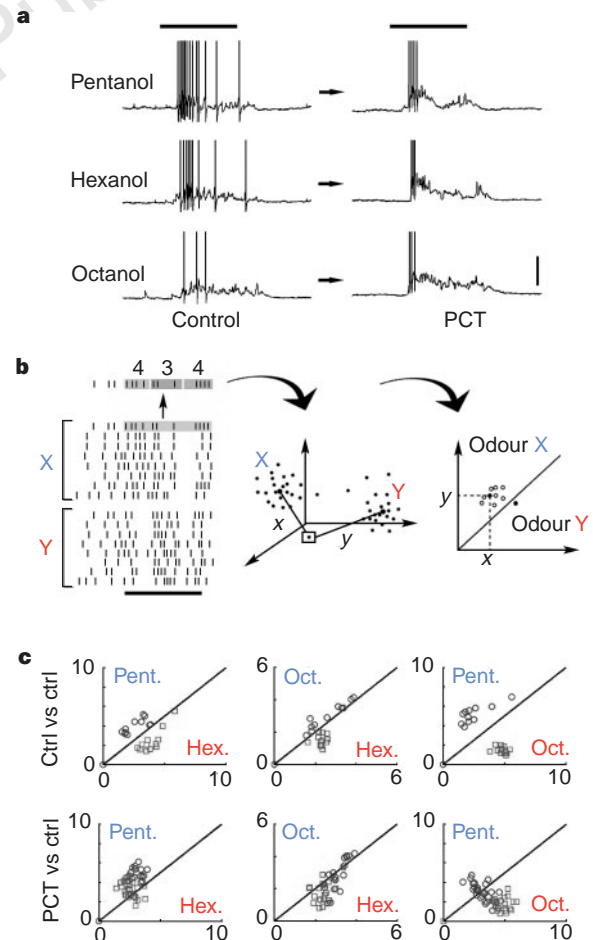


**Figure 3** Desynchronization of projection neurons causes loss of information in odour-evoked spike trains in single  $\beta$ -lobe neurons ( $\beta$ LN). **a**, Intracellular traces from one  $\beta$ LN in response to three odours before (control) and after picROTOXIN (PCT) treatment. Note the decrease in the difference between the three spike trains after PCT treatment. **b**, The clustering algorithm (method 1, Methods). **c**, Clustering algorithm (20-dimensional space) applied to control spike trains (top row) or post-PCT spike trains (bottom row) for the  $\beta$ LN in **a**. Diagonal line delineates classification, with results shown in Fig. 4a.

pairwise (and overall) classification now operated just above chance level (Figs 3c, bottom row and 4a, left). This indicates that picrotoxin induced both a shift in odour representation by the  $\beta$ -lobe neurons and a loss of information about stimulus identity in the temporal features of their spike trains. Among all  $\beta$ -lobe neurons for which there was good odour discriminability in controls ( $n = 14$   $\beta$ -lobe neurons;  $n = 34$  odour pairs), injection of picrotoxin hindered discrimination in eight  $\beta$ -lobe neurons for at least one odour pair in each neuron and for a total of nineteen odour pairs. In five of these eight neurons, discrimination was reduced to chance. Among all  $\beta$ -lobe neurons the probability of correct pairwise odour discrimination dropped from an average of  $\sim 90\%$  to  $\sim 75\%$  (Fig. 4b, left). A degradation was also found using

post-picrotoxin response patterns as templates (for example, Fig. 4a, left). Such discrimination was impaired (decreased by 10% or more) in seven  $\beta$ -lobe neurons ( $n = 9$  odour pairs) and reduced to chance in three.

To determine whether the information loss induced by picrotoxin in  $\beta$ -lobe neurons can be attributed to information loss in individual projection neurons, the same analysis was carried out with the projection neurons. A projection neuron (Fig. 5a), for example, responded to three odours with three distinct temporal patterns, allowing 93% correct odour identification in paired choices (Figs 4a, right and 5b, top row). After injection of picrotoxin into the antennal lobe, this projection neuron retained its original odour-specific response patterns, allowing a correct odour identification using either pre- or post-picrotoxin templates (Figs 4a, right and 5b, bottom row). In all the projection neurons thus tested, that showed above-chance odour discrimination before picrotoxin injection (16 odour/projection neuron pairs), injection of picrotoxin failed to alter pairwise odour discrimination using information contained in the projection neuron spike trains (Fig. 4b, right). A further comparison of odour classification by projection and  $\beta$ -lobe neurons was carried out using a clustering algorithm that preserves the continuous structure of the spike trains (see Methods). Over all  $\beta$ -lobe neurons ( $n = 19$ ) and odours (2.6 per neuron on average) tested, correct classification using this method dropped significantly from 67.6% to 40.1% (chance = 38.5%) after desynchronization of projection neurons (Fig. 4c, left). Over all projection neurons ( $n = 12$ ) and odours (2.9 on average per neuron) tested, odour

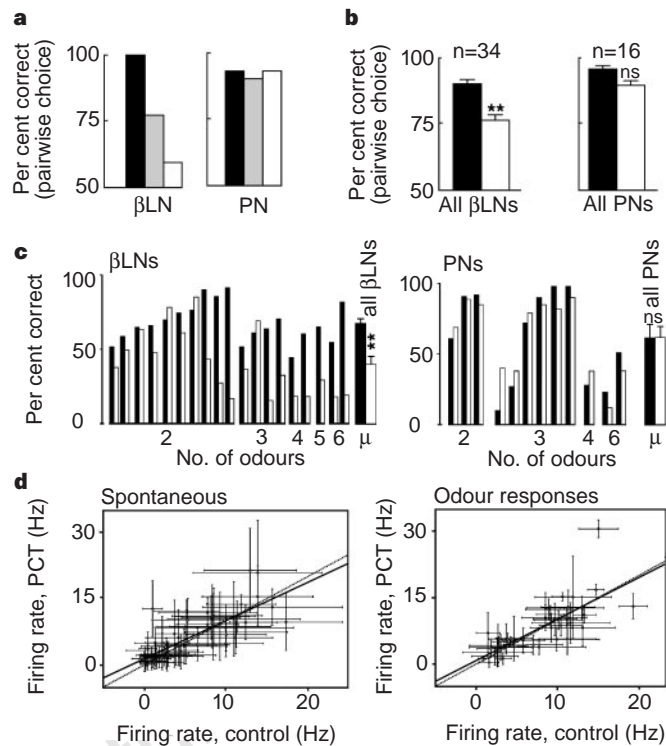


**Figure 4** Odour classification by  $\beta$ -lobe neurons (BLNs) and projection neurons (PNs) before and after picrotoxin (PCT) treatment. **a**, Categorization over all trials for the  $\beta$ LN in Fig. 3 and the PN in Fig. 5, using method 1. Black, control vs control; grey, PCT vs PCT; open, PCT vs control. Left, Perfect categorization of control trials (black, 72 correct out of 72) but impaired classification after PCT injection (grey, 147 of 190 trials; open, 113 of 190 trials). Right, PN shows an equally good categorization under all conditions (black, 112 of 120; grey, 121 of 134; open, 124 of 134). **b**, Summary of pairwise categorizations (method 1) for all BLNs (left) and PNs (right) with significant categorization of control trials. Black, control vs control; open, PCT vs control. Left, BLNs show a significant decrease in the percentage of correct categorization after PCT injection (\*\* $P < 0.005$ ). Right, PN performance is not significantly altered by PCT treatment. **c**, Categorization results using clustering method 2, applied to all BLNs (left) and all PNs (right) with significant categorization on control trials. 'Per cent correct' was calculated using all possible choices. BLNs and PNs are ranked on the abscissa according to the number of odours (2–6) to which they responded.  $\mu$  is the mean over all BLNs (left, \*\* $P < 0.0002$ ) and all PNs (right,  $P = 0.93$ , ns). Each neuron and  $\mu$  are represented by a pair of bars: black, control vs control; open, PCT vs control. **d**, PCT evokes no overall change in PN baseline (left,  $n = 54$  odour–neuron pairs) or odour-evoked (right,  $n = 38$  odour–neuron pairs) mean firing rates. Each point plots rate in one PN before ( $x$ -axis) vs after ( $y$ -axis) PCT injection. Rates (mean  $\pm$  s.d.) calculated over 1 s, from 8–30 trials from 26 PNs. We included only examples in which odour caused a response. Slope of linear regression fits: 0.86 (left,  $R = 0.8$ ); 0.94 (right,  $R = 0.76$ ).

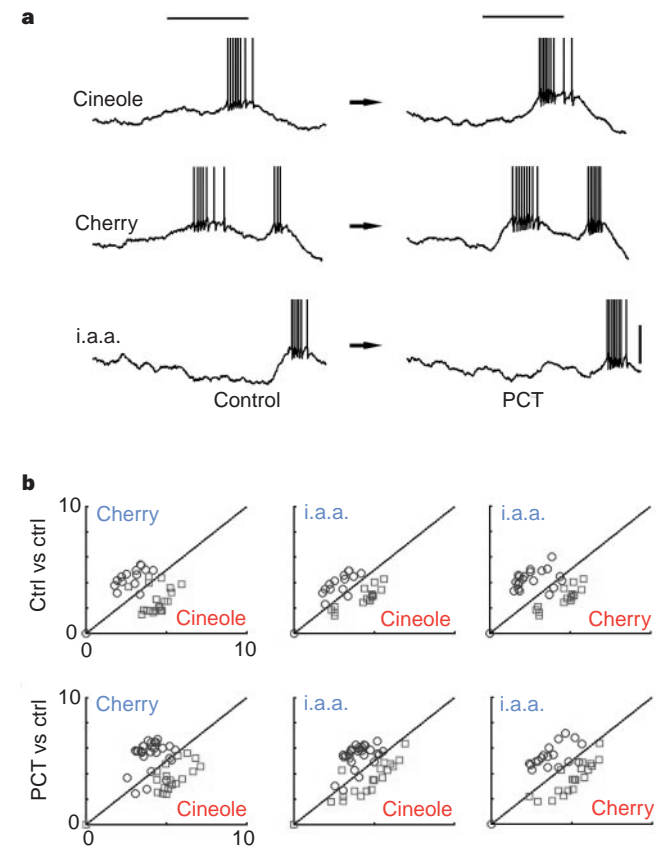


**Figure 5** Desynchronization of projection neurons (PNs) causes no loss of information in odour-evoked spike trains in single PNs. The same analysis as that in Fig. 3 was performed, but on a single PN. **a**, Note distinct response patterns to different odours (i.a.a., isoamylacetate) and their persistence after picrotoxin (PCT) treatment. **b**, Clustering algorithm (20-dimensional space) applied to control spike trains (top row) or post-PCT spike trains (bottom row) for the PN in **a**. Classification results are shown in Fig. 4a.

classification was unaffected after desynchronization of projection neurons (control, 61.8% correct; picrotoxin, 62.1% correct) (Fig. 4c, right). Finally, we quantified the effects of picrotoxin injection on the spontaneous and stimulus-evoked firing rates of 26 projection neurons. These results indicated unchanged projection neuron rates in post-picrotoxin trials (Fig. 4d).

Thus, we have identified a population of central olfactory neurons that can be used as a neural 'read-out' of population activity in the antennal lobe. The tuning of these  $\beta$ -lobe neurons was affected by desynchronization of projection neurons induced by picrotoxin in two principal ways, which were never observed in individual projection neurons. First, odour discrimination using information contained in the spike trains of  $\beta$ -lobe neurons became less likely (often reduced to chance) after picrotoxin treatment. These effects were odour-specific and could affect the responses to related chemical stimuli, blurring their specific differences. Second, picrotoxin-induced desynchronization of projection neurons could cause the induction of new, but not generalized, odour responses in  $\beta$ -lobe neurons. Because these effects were never observed in projection neurons, we propose that they were induced by desynchronization of projection neurons and that  $\beta$ -lobe neurons (and perhaps the neurons presynaptic to them) are sensitive to the temporal structure of their inputs. Our earlier behavioural study indicated that treatment with picrotoxin impairs fine odour discrimination<sup>15</sup>. Our present results indicate that behavioural impairments may be due to a partial loss of stimulus-related information in neurons involved in processing information between early and higher olfactory centers. We thus propose that neural synchronization is indeed important for information processing in the brain: it is, at least partly, a temporal substrate for the transmission of information that is contained across co-activated neurons (relational code). Such information cannot be retrieved by simple averaging of the input channels' activities without considering their temporal relationships. It will be interesting to determine whether such coding principles apply to other systems endowed with neuronal synchronization. □

## Methods

**Electrophysiology.** Sixty-three adult non-anaesthetized male locusts (*Schistocerca americana*) were taken from a crowded colony and immobilized with one antenna intact and exposed for stimulation, as described<sup>18</sup>. Intracellular recordings were made from the soma or dendrites of 26 antennal lobe projection neurons and from the dendrites of 37  $\beta$ -lobe neurons by using glass micropipettes<sup>18</sup>. Intracellular staining was carried out by iontophoretic injection of 6% cobalt hexamine (0.5–2 nA, 1 Hz). Histology and intensification were performed as in ref. 23.  $\beta$ -lobe neurons may be homologous to multimodal neurons described in other insect species<sup>21,22</sup>. Local field potentials were recorded with saline-filled patch pipettes from the mushroom body calyx. Picrotoxin was applied locally to the antennal lobe neuropil by pressure injection<sup>19</sup>. Glass capillaries were back-filled with a 0.1 M saline solution of picrotoxin and injected volumes were ~1 pl. Controls for absence of picrotoxin leakage outside the antennal lobe were carried out by dye injection. Controls for absence of mechanical effects of drug injection were done by testing eight  $\beta$ -lobe neurons before and after injection of saline in the antennal lobe. In a few experiments with projection neurons, picrotoxin was bath-applied, which was shown previously to have the same effects on them as pressure-injection<sup>19</sup>. Bath application of picrotoxin was never used with  $\beta$ -lobe neurons. Electrophysiological data were digitized at 5 kHz post-hoc from DAT with LabVIEW software and an NBMIO16L interface (National Instruments). Data were analysed with MATLAB (Mathworks). Airborne odours were delivered to an antenna as described<sup>18</sup>.

**Test for induced responses.** For each set of trials (odour, condition) we calculated a mean  $\pm$  s.e.m. smooth peristimulus time histogram (PSTH) by convolving each raster with a 25-ms Gaussian and summing the results. We then calculated, for each time  $t$  (1-ms resolution), whether the firing rate during the response (for 2 s after odour onset) was different from the mean baseline firing rate (for 1 s before odour onset) by at least 2 s.e.m. for at least 100

contiguous ms. The response was described as different between pre- and post-picrotoxin injection if a significant ( $P < 0.05$ , unpaired two-tailed  $t$ -test) difference between corresponding epochs occurred. Changes so measured could thus occur over multiple epochs within a response (Fig. 2d). This method ensured the detection of brief responses or ones that include both excitation and inhibition.

**Cluster analysis, method 1.** Methods 1 and 2 were used with all  $\beta$ -lobe and projection neurons that responded to two or more of the ten odours presented. With method 1, odour discriminations were tested pairwise (for example, four odours meant six pairwise comparisons). Each spike train in a set (one set for each pre- and post-picrotoxin condition and odour condition) was divided into  $n$  non-overlapping bins over the 2-s post-stimulus onset period. The spike count in each bin was used to construct an  $n$ -dimensional vector representing this trial. The operation was repeated with each trial in the set, to form a cluster. We tested bin sizes between 10 and 1,800 ms, and found optimal clustering in most experiments for 50–200 ms and least clustering below 10 ms or above 1,200 ms (approximately average firing rate). We present data for 100-ms bins, and thus  $n = 20$ . The objective was to assess the separation between two clusters (for example, between the X and Y clusters), by assigning each spike train (or vector) one likely stimulus on the basis of its Euclidian distance to the centre of each of the two clusters. For each pairwise comparison, therefore, each trial produced two numbers (for example, distances  $x$  and  $y$  to the centres of the X and Y clusters), which were plotted against each other (Fig. 3b). The per cent of correct classification over all trials was given by the proportion of points that fell on the 'correct' side of the diagonal. Significance of the 'per cent correct classification' was calculated by finding its binomial probability, given a forced choice (threshold  $P < 0.05$ ; paired one-tailed  $t$ -tests). Control trials were compared to control (1) and to picrotoxin (2) trials (Figs 3c and 5b). Picrotoxin trials were compared to picrotoxin trials (3) (not shown). Comparison (1) describes the classification of odour responses in control conditions. Comparison (2) describes the classification of post-picrotoxin odour responses based on their control templates. This comparison best assesses the information loss caused by input desynchronization. Comparison (3) describes the classification of post-picrotoxin odour responses based on their post-picrotoxin templates.

**Cluster analysis, method 2.** This clustering analysis is based on the cost-based metric methods<sup>24</sup> according to which a 'distance' is computed between spike trains. This distance is defined as the cost paid to transform one spike train into the other using three elementary steps: insertion; deletion of a spike (each at a cost of 1); and displacement of a spike by 1 ms (cost of  $2/T$  for each displacement, where  $T$  is the maximum separation in ms allowed between the spike time in one train and that in the other). We used a range for  $T$  between 16 and 4,000, with  $T = 150$  providing the best classification overall, as with method 1. Results were not greatly different for  $16 < T < 1,000$ . Classification was similar whether the mean was arithmetic (all points equal) or geometric (less weight to outliers). Per cent correct in Fig. 4c results from choosing among all odours without restriction to pairwise assignments in those neurons that responded to more than two odours. For each neuron  $i$ , chance level is thus  $1/m_i$ , where  $m_i$  is the number of odours to which neuron  $i$  responded. The effective number of odours in the plots of  $\mu$  (Fig. 4c) is calculated as  $((1/m_i))^{-1}$ . We used paired two-tailed  $t$ -tests to measure significance.

Received 5 June; accepted 10 August 1998.

- Mountcastle, V. B. Modality and topographic properties of single neurons of cat's somatic sensory cortex. *J. Neurophysiol.* **20**, 408–434 (1957).
- Sparks, D. L., Lee, C. & Rohrer, W. H. Population coding of the direction, amplitude and velocity of saccadic eye movements by neurons in the superior colliculus. *Cold Spring Harb. Symp. Quant. Biol.* **55**, 805–811 (1990).
- Georgopoulos, A. P., Lurito, J. T., Petrides, M., Schwartz, A. B. & Massey, J. T. Mental rotation of the neuronal population vector. *Science* **243**, 234–236 (1989).
- Newsome, W. T., Britten, K. H. & Movshon, J. A. Neuronal correlates of a perceptual decision. *Nature* **341**, 52–54 (1989).
- Abbott, L. F. Decoding neuronal firing and modeling neural networks. *Q. Rev. Biophys.* **27**, 291–331 (1994).
- Abeles, M., Bergman, H., Margalit, E. & Vaadia, E. Spatiotemporal firing patterns in the frontal cortex of behaving monkeys. *J. Neurophysiol.* **70**, 1629–1638 (1993).
- Gray, C. M. & Singer, W. Stimulus-specific neuronal oscillations in orientation columns of cat visual cortex. *Proc. Natl Acad. Sci. USA* **86**, 1698–1702 (1989).
- Roelfsema, P., Engel, A. K., König, P. & Singer, W. The role of neuronal synchronization in response selection: a biologically plausible theory of structural representations in the visual cortex. *J. Cog. Neurosci.* **8**, 603–625 (1996).
- Fries, P., Roelfsema, P., Engel, A. K., König, P. & Singer, W. Synchronization of oscillatory responses in visual cortex correlates with perception in interocular rivalry. *Proc. Natl Acad. Sci. USA* **94**, 12699–12704 (1997).

10. Riehle, A., Grün, S., Diesmann, M. & Aertsen, A. Spike synchronization and rate modulation differentially involved in motor cortical function. *Science* **278**, 1950–1953 (1997).
11. Nicoletti, M. A. L., Baccala, L. A., Lin, R. C. S. & Chapin, J. K. Sensorimotor encoding by synchronous neural ensemble activity at multiple levels of the somatosensory system. *Science* **268**, 1353–1358 (1995).
12. Milner, P. A model for visual shape recognition. *Psychol. Rev.* **81**, 521–535 (1974).
13. von der Malsburg, C. *The Correlation Theory of Brain Function* (Internal report, Max-Planck-Inst. Biophys. Chem., Göttingen, 1981).
14. Singer, W. Synchronization of cortical activity and its putative role in information processing and learning. *Annu. Rev. Physiol.* **55**, 349–374 (1993).
15. Stopfer, M., Bhagavan, S., Smith, B. H. & Laurent, G. Impaired odour discrimination on desynchronization of odour-encoding assemblies. *Nature* **390**, 70–74 (1997).
16. Wehr, M. & Laurent, G. Odour encoding by temporal sequences of firing in oscillating neural assemblies. *Nature* **384**, 162–166 (1996).
17. Laurent, G. & Davidowitz, H. Encoding of olfactory information with oscillating neural assemblies. *Science* **265**, 1872–1875 (1994).
18. Laurent, G., Wehr, M. & Davidowitz, H. Temporal representation of odours in an olfactory network. *J. Neurosci.* **16**, 3837–3847 (1996).
19. MacLeod, K. & Laurent, G. Distinct mechanisms for synchronization and temporal patterning of odour-encoding neural assemblies. *Science* **274**, 976–979 (1996).
20. Laurent, G. & Naraghi, M. Odorant-induced oscillations in the mushroom bodies of the locust. *J. Neurosci.* **14**, 2993–3004 (1994).
21. Homberg, U. Processing of antennal information in extrinsic mushroom body neurons of bee brain. *J. Comp. Physiol. A* **154**, 825–836 (1984).
22. Li, Y. & Strausfeld, N. Morphology and sensory modality of mushroom body extrinsic neurons in the brain of the cockroach, *Periplaneta americana*. *J. Comp. Neurol.* **387**, 631–650 (1997).
23. Bacon, J. P. & Altman, J. S. A silver intensification method for cobalt-filled neurones in wholemount preparations. *Brain Res.* **138**, 359–363 (1977).
24. Victor, J. D. & Purpura, K. P. Metric-space analysis of spike trains: theory, algorithms and application. *Network Comp. Neural Syst.* **8**, 127–164 (1997).
25. Leitch, B. & Laurent, G. GABAergic synapses in the antennal lobe and mushroom body of the locust olfactory system. *J. Comp. Neurol.* **373**, 487–514 (1996).

**Acknowledgements.** We thank E. M. Schuman and C. Koch for comments on the manuscript, and the members of the Laurent laboratory for constructive criticism during this work. This work was supported by NSF and NIDCD grants (to G.L.), the Sloan Center for Neuroscience at Caltech and an NIH training grant.

Correspondence and requests for materials should be addressed to G.L. (e-mail: laurentg@cco.caltech.edu).

## Destabilization of $\beta$ -catenin by mutations in presenilin-1 potentiates neuronal apoptosis

Zhuohua Zhang\*, Henrike Hartmann\*, Viet Minh Do\*, Dorothee Abramowski†, Christine Sturchler-Pierrat†, Matthias Staufenbiel‡, Bernd Sommer‡, Marc van de Wetering‡, Hans Clevers‡, Paul Saftig§, Bart De Strooper||, Xi He\* & Bruce A. Yankner\*

\* Department of Neurology, Harvard Medical School and Division of Neuroscience, The Children's Hospital, 300 Longwood Avenue, Boston, Massachusetts 02115, USA

† Preclinical Research, Novartis Pharma Ltd, CH-4002 Basel, Switzerland

‡ Department of Immunology, University Hospital, 3508 GA Utrecht, The Netherlands

§ Zentrum Biochemie und Molekular Zellbiologie, Abteilung Biochemie II, Universität Göttingen, 37073 Göttingen, Germany

|| Flemish Institute for Biotechnology (VIB4), Center for Human Genetics, K.U. Leuven, B-3000 Belgium

Mutations of the presenilin-1 gene are a major cause of familial early-onset Alzheimer's disease<sup>1–4</sup>. Presenilin-1 can associate with members of the catenin family of signalling proteins, but the significance of this association is unknown<sup>5,6</sup>. Here we show that presenilin-1 forms a complex with  $\beta$ -catenin *in vivo* that increases  $\beta$ -catenin stability. Pathogenic mutations in the presenilin-1 gene reduce the ability of presenilin-1 to stabilize  $\beta$ -catenin, and lead to increased degradation of  $\beta$ -catenin in the brains of transgenic mice. Moreover,  $\beta$ -catenin levels are markedly reduced in the brains of Alzheimer's disease patients with presenilin-1 mutations. Loss of  $\beta$ -catenin signalling increases neuronal vulnerability to apoptosis induced by amyloid- $\beta$  protein. Thus, mutations in presenilin-1 may increase neuronal apoptosis by altering the

## stability of $\beta$ -catenin, predisposing individuals to early-onset Alzheimer's disease.

To determine whether presenilin-1 (PS1) interacts with  $\beta$ -catenin in a physiological complex, we studied immunoprecipitates of endogenous PS1 from human cell lines and brain for the presence of  $\beta$ -catenin. Antibodies against both the amino- and the carboxy-terminal domains of PS1 (PS1-N and PS1-C)<sup>7</sup> precipitated both PS1 and  $\beta$ -catenin in every cell line studied and in human brain (Fig. 1a, b). We confirmed the specificity of immunoprecipitation of PS1 by pre-absorption of the PS1-N and PS1-C antibodies with their cognate antigens (Fig. 1b), and by immunoprecipitations with PS1 preimmune serum or with an antibody to SREBP-1, which is, like PS1, a transmembrane protein of the endoplasmic reticulum (Fig. 1d).

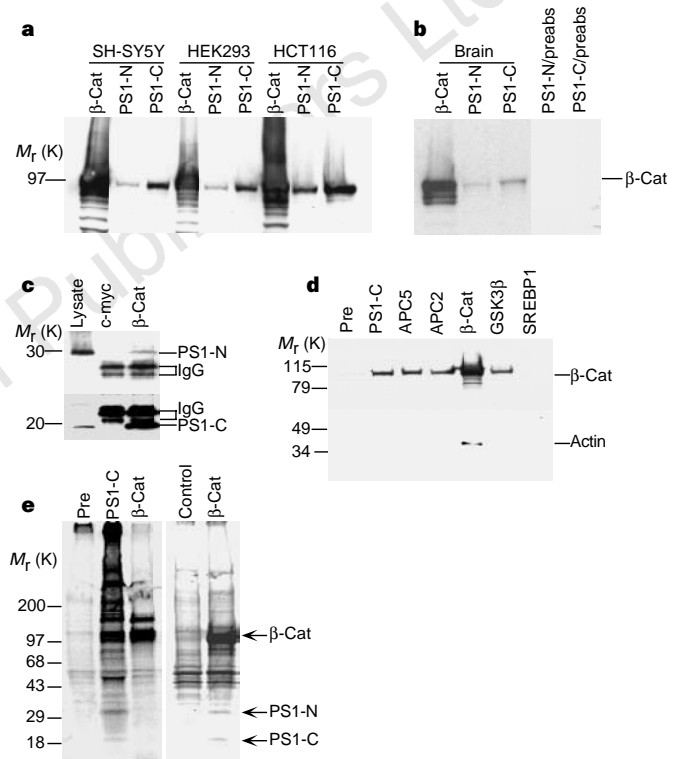


**Figure 1** Native complex formation between  $\beta$ -catenin and PS1. **a**, Co-precipitation of  $\beta$ -catenin with PS1 in neuroblastoma SH-SY5Y, HEK293 and HCT116 cells. Protein-equivalent cell lysates were immunoprecipitated with antibodies against  $\beta$ -catenin ( $\beta$ -Cat), the PS1 N terminus (PS1-N), or the PS1 C-terminal loop domain (PS1-C), and then analysed for  $\beta$ -catenin by immunoblotting with an anti- $\beta$ -catenin monoclonal antibody (mAb14). The immunoprecipitating antibodies are indicated above each lane and the immunoblotting antibodies are indicated at the right of **b**. **b**, Co-precipitation of  $\beta$ -catenin with PS1 in brain. Pre-absorption of the anti-PS1 antibodies by their cognate antigens abolishes co-precipitation of  $\beta$ -catenin (PS1-N/preabs, PS1-C/preabs). **c**, Co-precipitation of the PS1 N- and C-terminal fragments with  $\beta$ -catenin. HCT116 cell lysates were immunoprecipitated with a control antibody (c-Myc) or with anti- $\beta$ -catenin ( $\beta$ -Cat), followed by immunoblotting with anti-PS1-N (upper panel) or anti-PS1-C (lower panel). Immunoblotting of the whole-cell lysate shows the positions of the PS1 N- and C-terminal fragments (PS1-N and PS1-C; upper and lower panels, respectively). The IgG light chain from the immunoprecipitation is indicated. **d**, Comparative co-precipitation of PS1,  $\beta$ -catenin, GSK-3 $\beta$  and APC. Immunoprecipitations of protein-equivalent lysates of SW480 cells were done with preimmune PS1 serum (Pre), or with the indicated antibodies, followed by immunoblot analysis for  $\beta$ -catenin or actin. **e**, Stoichiometric relation of PS1 to  $\beta$ -catenin in PS1- $\beta$ -catenin complexes. COS cells co-transfected with  $\beta$ -catenin and PS1 (left panel) or non-transfected SW480 cells (right panel) were metabolically labelled with [<sup>35</sup>S]methionine and immunoprecipitated with the indicated antibodies. The co-precipitated PS1 N- and C-terminal fragments and  $\beta$ -catenin are shown. A stoichiometry of 2 : 1 (PS1-C :  $\beta$ -catenin) was determined for both cell types.